

# The Causes and Implications of Persistent Atmospheric Carbon Dioxide Biases in Earth System Models

Forrest M. Hoffman<sup>†‡</sup>, James T. Randerson<sup>†</sup>, and CMIP5 Carbon Cycle Model Leads

<sup>†</sup>Department of Earth System Sciences, University of California, Irvine, CA;

<sup>‡</sup>Computational Earth Sciences Group, Oak Ridge National Laboratory, Oak Ridge, TN

## Introduction

Increasing atmospheric carbon dioxide ( $\text{CO}_2$ ) concentrations, resulting from anthropogenic perturbation of the global carbon cycle, are altering the Earth's climate. The strength of feedbacks between a changing climate and future  $\text{CO}_2$  concentrations are highly uncertain and difficult to predict using Earth System Models (ESMs). To reduce the range of uncertainty in climate predictions, model representation of feedbacks must be improved through comparisons with contemporary observations. In this study, we analyzed emissions-driven simulations for historical (1850–2005) and future periods (Representative Concentration Pathway or RCP 8.5 for 2006–2100) produced by 13 ESMs for the Fifth Phase of the Coupled Model Intercomparison Project (CMIP5). We exploited a linear relationship found between the magnitude of contemporary and future atmospheric  $\text{CO}_2$  levels to create a contemporary  $\text{CO}_2$  tuned model (CCTM) estimate of the trajectory for the 21<sup>st</sup> century. This approach reduced the spread of future atmospheric  $\text{CO}_2$  projections by a factor of 6.4 at 2060 and yielded radiative forcing and temperature increases during the 21<sup>st</sup> century that were lower than the multi-model mean.

## Description of Models

Table 1: Models that generated output used in this study.

Model	Modeling Center (or Group)	Atmosphere	Component Models and Resolutions	Ocean	Snow/Ice
BCC-CSM1.1	Beijing Climate Center, China Meteorological Administration, CHINA	AGCM2.1 (T42L26)	AVIM1.0 (T42)	MOM4.1 (tripolar, $1^\circ \times (1-\frac{1}{3})^\circ, L40$ )	SIS (tripolar, $1^\circ \times (1-\frac{1}{3})^\circ, L40$ )
BCC-CSM1.1(m)	Beijing Climate Center, China Meteorological Administration, CHINA	AGCM2.1 (T42L26)	AVIM1.0 (T42)	MOM4.1 (tripolar, $1^\circ \times (1-\frac{1}{3})^\circ, L40$ )	SIS (tripolar, $1^\circ \times (1-\frac{1}{3})^\circ, L40$ )
BNU-ESM <sup>a</sup>	Beijing Normal University, CHINA	CAM3.5 (T42L26)	CoLM + BNUDGVM	MOM4P1 (360 $\times$ 200, L50)	CICE4.1 (360 $\times$ 200)
CanESM2 <sup>b</sup>	Canadian Centre for Climate Modelling and Analysis, CANADA	CanAM4 (T63L35)	CLM2.7 and CTM1	CanCM4 (256 $\times$ 192, L40) and CMOC1.2	CanSIM1 (T63)
CESM1-BGC	Community Earth System Model Consortium, NSF-DOE/NCAR, USA	CM4 (0.9 $\times$ 1.25°)	CLM4 (0.9 $\times$ 1.25°)	POP2 (gx1v6)	CICE (gx1v6)
GFDL-ESM2g, GFDL-ESM2m <sup>c</sup>	NOAA Geophysical Fluid Dynamics Laboratory, USA	AM2 (2 $\times$ 2.5°, L24)	LM3	MOM2 (tripolar, $1^\circ \times (1-\frac{1}{3})^\circ, L50$ )	SIS (tripolar, $1^\circ \times (1-\frac{1}{3})^\circ, L50$ )
HadGEM2-ES <sup>d</sup>	Met Office Hadley Centre, UNITED KINGDOM	HadGAM2 and UKCA (N68L38)	MOSES2 and TRIFFID	HadGOM2 and diaH-OC2 (1 $\times$ (1- $\frac{1}{3}$ )°, L40)	—
INM-CM4 <sup>e</sup>	Institute for Numerical Mathematics, RUSSIA	(2 $\times$ 1.5°, L21)	—	—	—
IPSL-CM5A-LR <sup>f</sup>	Institut Pierre-Simon Laplace, FRANCE	LMDZ4 (3.75 $\times$ 1.9°, L39)	ORCHIDEE	ORCA2 and PISCES (2 $\frac{1}{2}$ $\times$ (2- $\frac{1}{2}$ )°, L31)	LIM2
MRC-ESM <sup>g</sup>	Japan Agency for Marine-Earth Sciences and Technology, Atmosphere and Ocean Research Institute (The University of Tokyo), and National Institute of Environmental Studies, JAPAN	MIROC-AGCM and SPINTARS (T42L20)	MATSIRO and SEIB-DGM (T42, L6)	COCO3.0 and NPZD (256 $\times$ 192, L44)	COCO3.4
MIPE-ESM <sup>h</sup>	Max Planck Institute for Meteorology, GERMANY	ECHAM6 (16S47)	JSBACH	MIPCM and HAMOCC (1 $\times$ 0.5°, L40)	4936
MRI-ESM <sup>i</sup>	Meteorological Research Institute, JAPAN	GSMUV (TL159L48)	HAL and MRI-LCCM2	MRI-COM3 (1 $\times$ 0.5°, L51)	MRI-COM3
Nakano et al., 2011	—	—	—	—	—

<sup>a</sup>Atmospheric CO<sub>2</sub> required unit correction.

<sup>b</sup>GFDL-ESM2g and GFDL-ESM2m output available beginning January 1861.

<sup>c</sup>Ocean carbon flux required unit correction.

<sup>d</sup>HadGEM2-ES output available for December 1859 through November 2009; annual atmospheric CO<sub>2</sub> obtained directly from Hadley Centre.

<sup>e</sup>BNU-ESM provided no ocean cell area data.

<sup>f</sup>IPSL-CM5A-LR monthly atmospheric CO<sub>2</sub> obtained directly from IPSL-CM5A-LR.

<sup>g</sup>IPSL-CM5A-LR provided three esmHistorical realizations and one esmProject realization.

## Observations and Calculations

- We used an observationally based estimate of anthropogenic CO<sub>2</sub> uptake by the ocean, produced by Khatiwala et al. (2009, 2012) using a Green's function model for ocean tracer transport, in combination with observed atmospheric CO<sub>2</sub> and fossil fuel emission estimates to assess model biases in carbon accumulation in the atmosphere, ocean, and land reservoirs.
- We adopted a strategy similar to that of Hall and Qu (2006) to constrain future trends in atmospheric CO<sub>2</sub> using contemporary observations to create the CCTM.
- We employed an impulse response function to estimate temperature changes based on time-integrated changes in radiative forcing to evaluate the implications of model CO<sub>2</sub> biases.

## Contemporary Biases in Atmospheric CO<sub>2</sub>

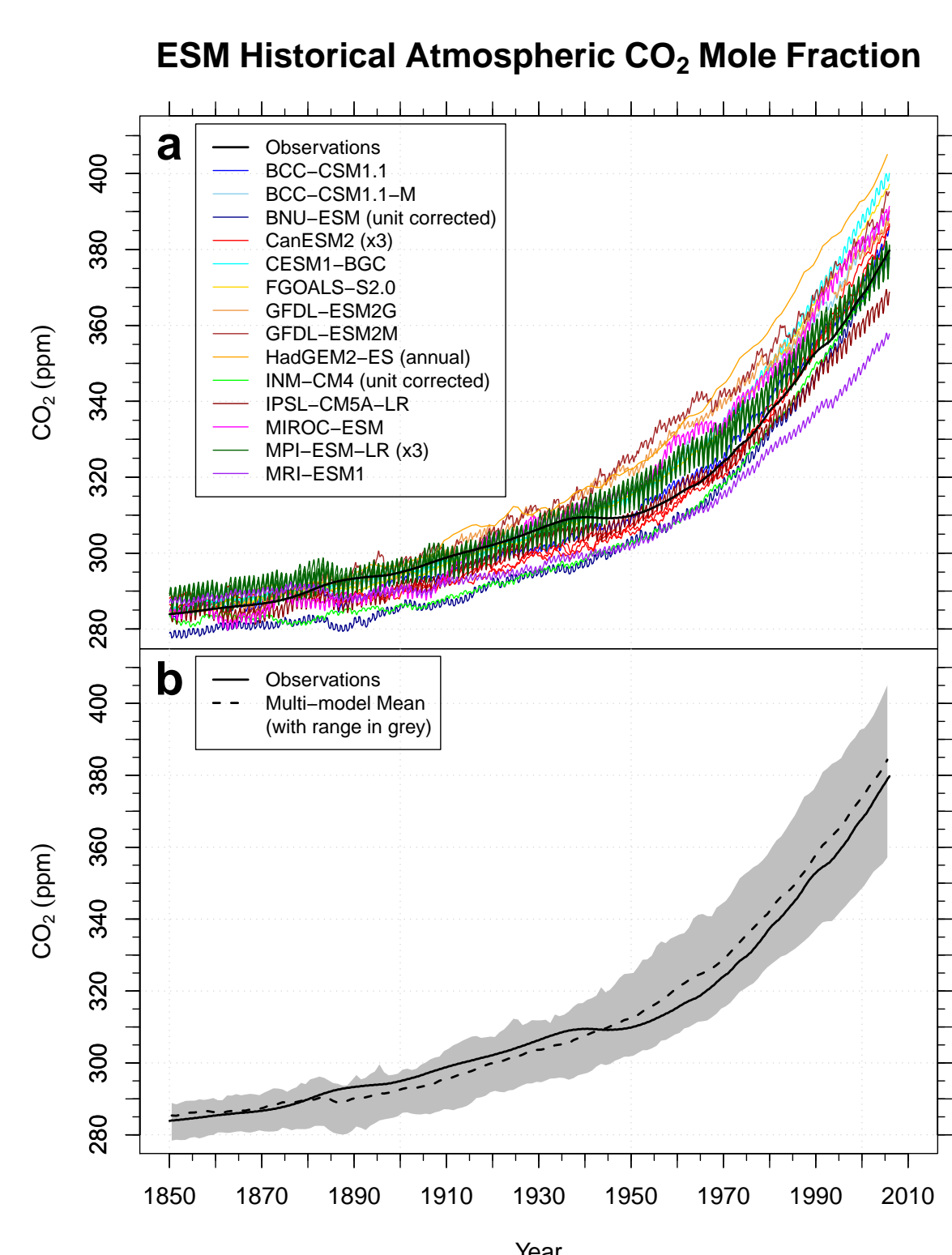


Figure 1: (a) Most ESMs exhibit a high bias in atmospheric CO<sub>2</sub> mole fraction. (b) The multi-model mean is biased high from 1945 throughout the 20<sup>th</sup> century, ending 5.3 ppm above observations in 2005.

## ESM Historical Ocean and Land Carbon Accumulation

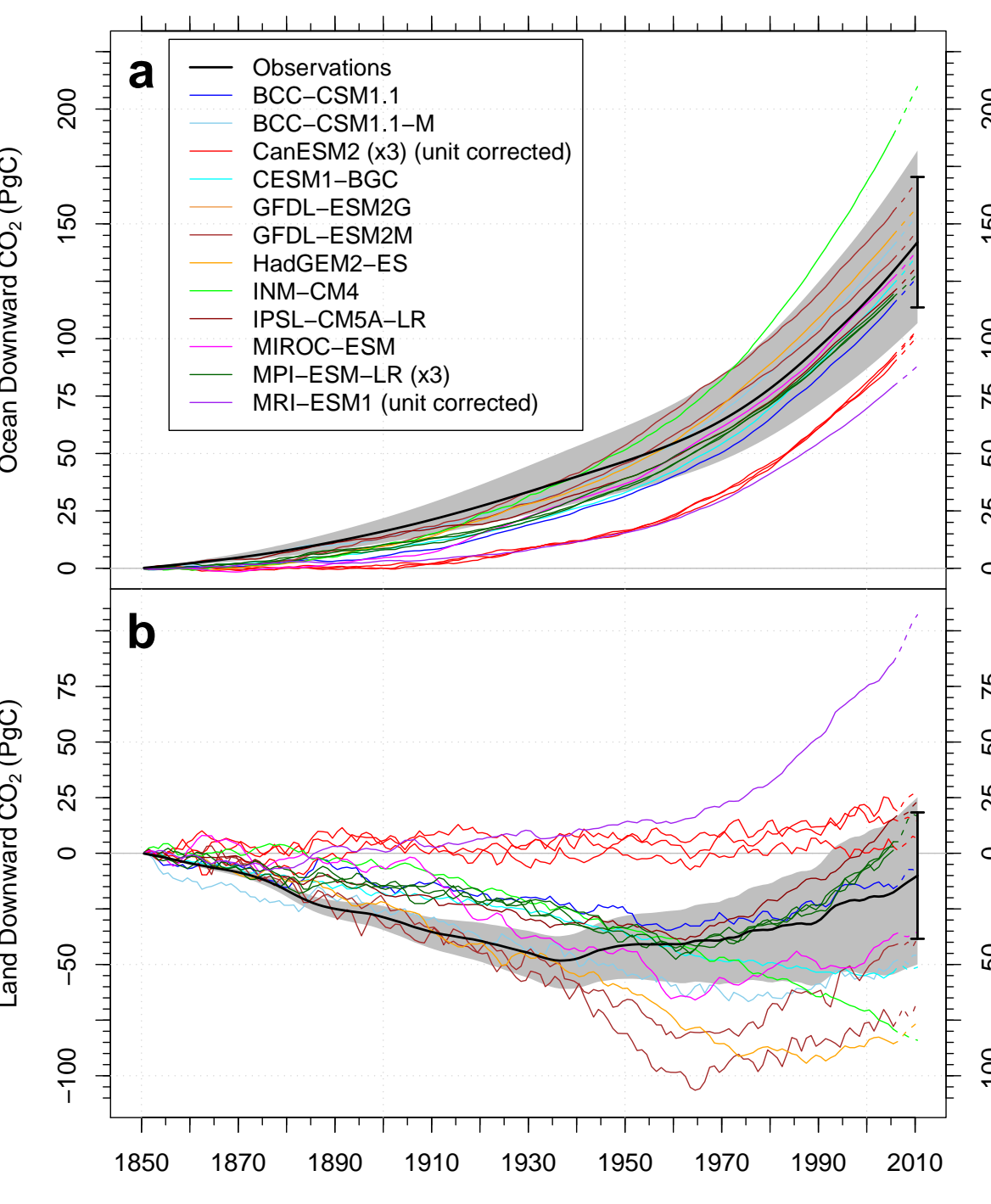


Figure 2: (a) Ocean carbon accumulation from CMIP5 models ranged from 55–325 Pg C in 2010 as compared with adjusted estimates from Khatiwala et al. (2009, 2012). (b) CMIP5 models exhibit a wide range of land carbon accumulation responses, ranging from a cumulative net source of 125 Pg C to a sink of 75 Pg C in 2010.

## Causes and Implications of the Contemporary Bias

- A key driver of the persistent high bias was weak ocean carbon uptake exhibited by the majority of ESMs.
- The high atmospheric CO<sub>2</sub> bias for the multi-model mean produced radiative forcing that was too large and, consequently, an unrealistically high temperature increase during the historical period.
- We will see that the atmospheric CO<sub>2</sub> bias persists into the future, causing large and divergent model projections during the 21<sup>st</sup> century.

## Comparison with Khatiwala et al. (2009, 2012)

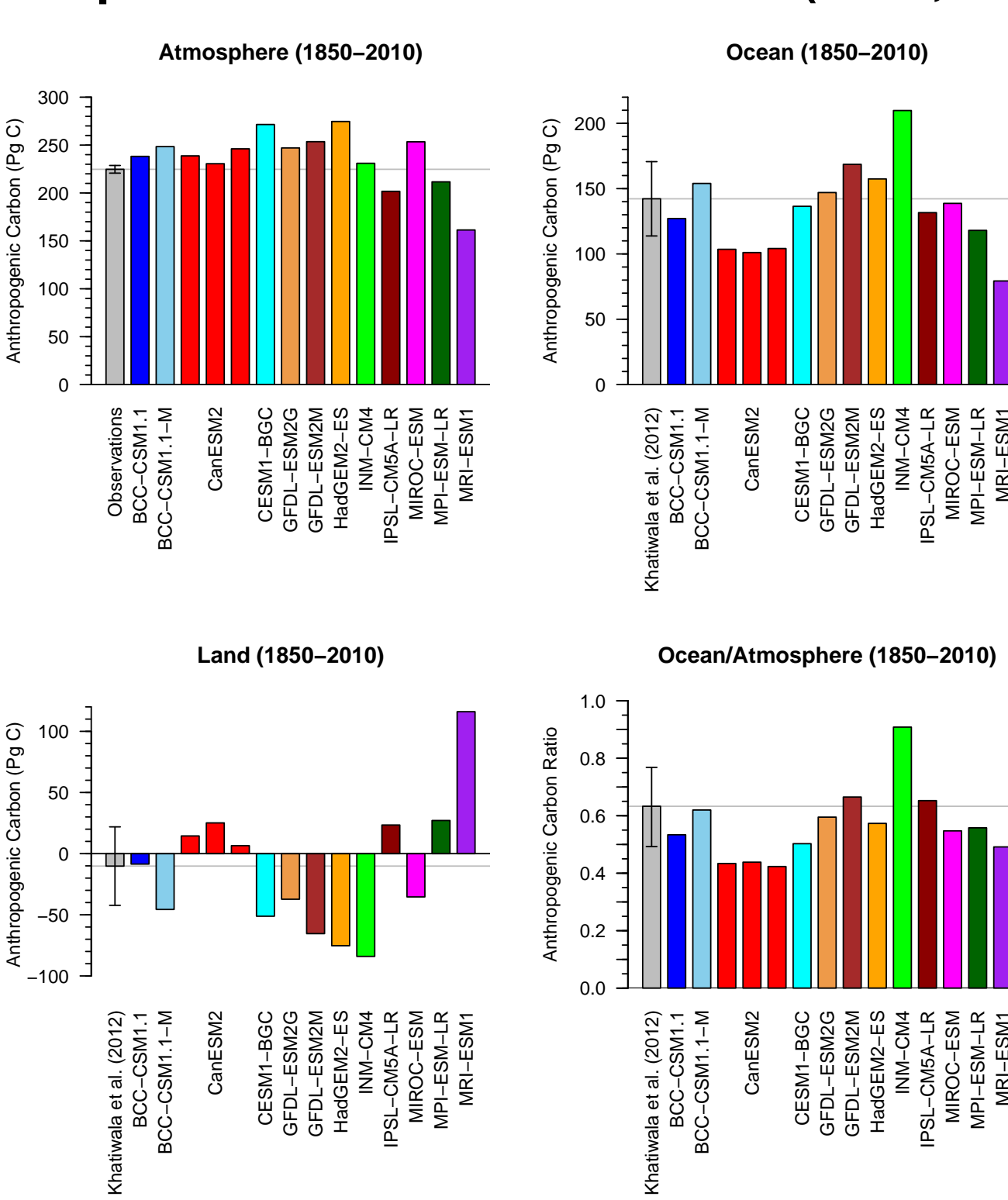


Figure 3: Reconstructed atmospheric CO<sub>2</sub> levels and observationally based estimates of carbon uptake from Khatiwala et al. (2009, 2012) provide powerful constraints on carbon inventories in the atmosphere and ocean as well as on land. While ocean carbon accumulation appears adequate in some model results, ocean carbon accumulation in most ESMs show a low bias once normalized by atmospheric accumulation (lower right panel).

## Persistence of Biases into the Future

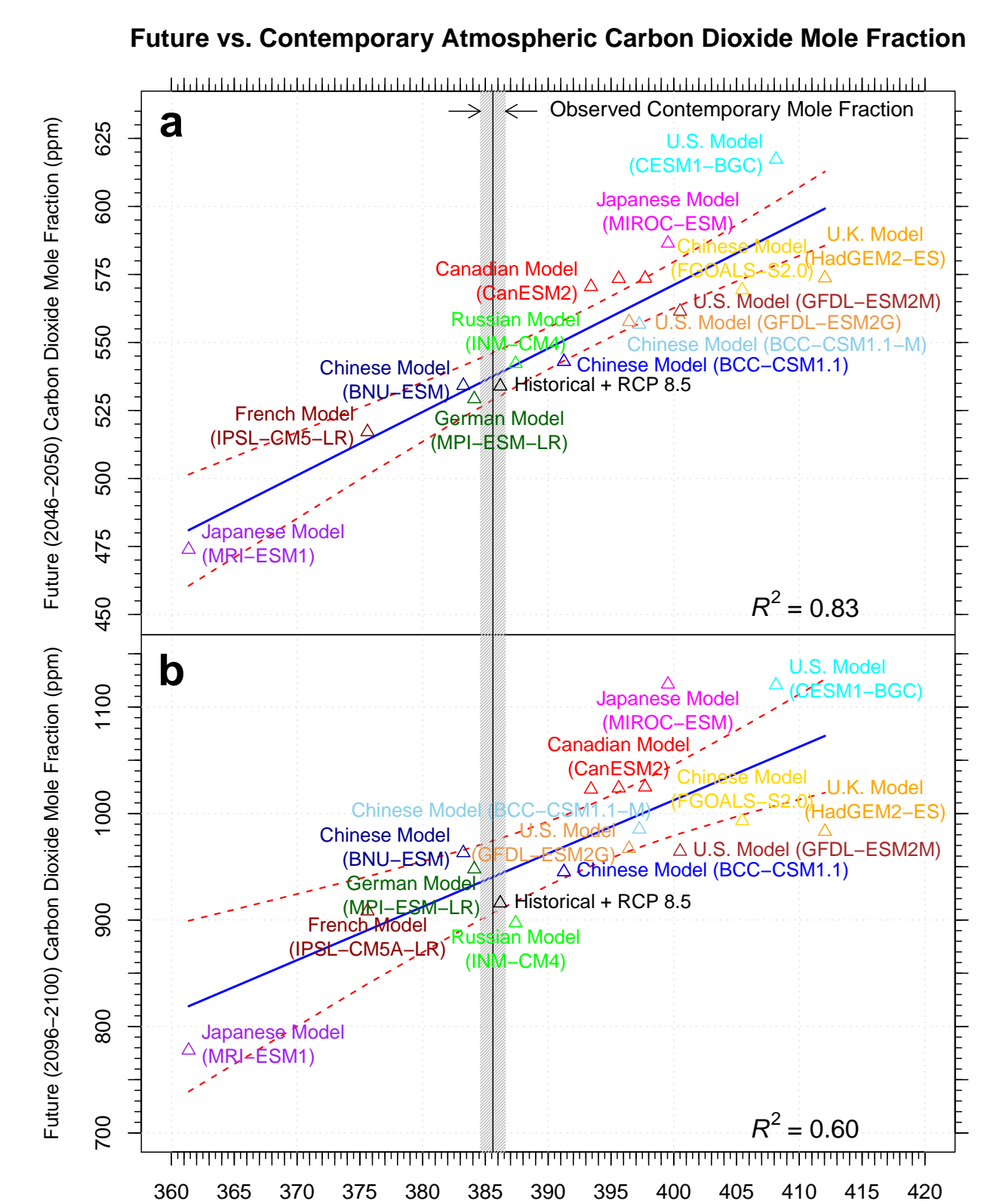


Figure 4: (a) Future (2050) vs. contemporary (2010) atmospheric CO<sub>2</sub> mole fraction fit for CMIP5 emissions-forced simulations of RCP 8.5. (b) Future (2100) vs. contemporary (2010) atmospheric CO<sub>2</sub> mole fraction fit for CMIP5 emissions-forced simulations of RCP 8.5.

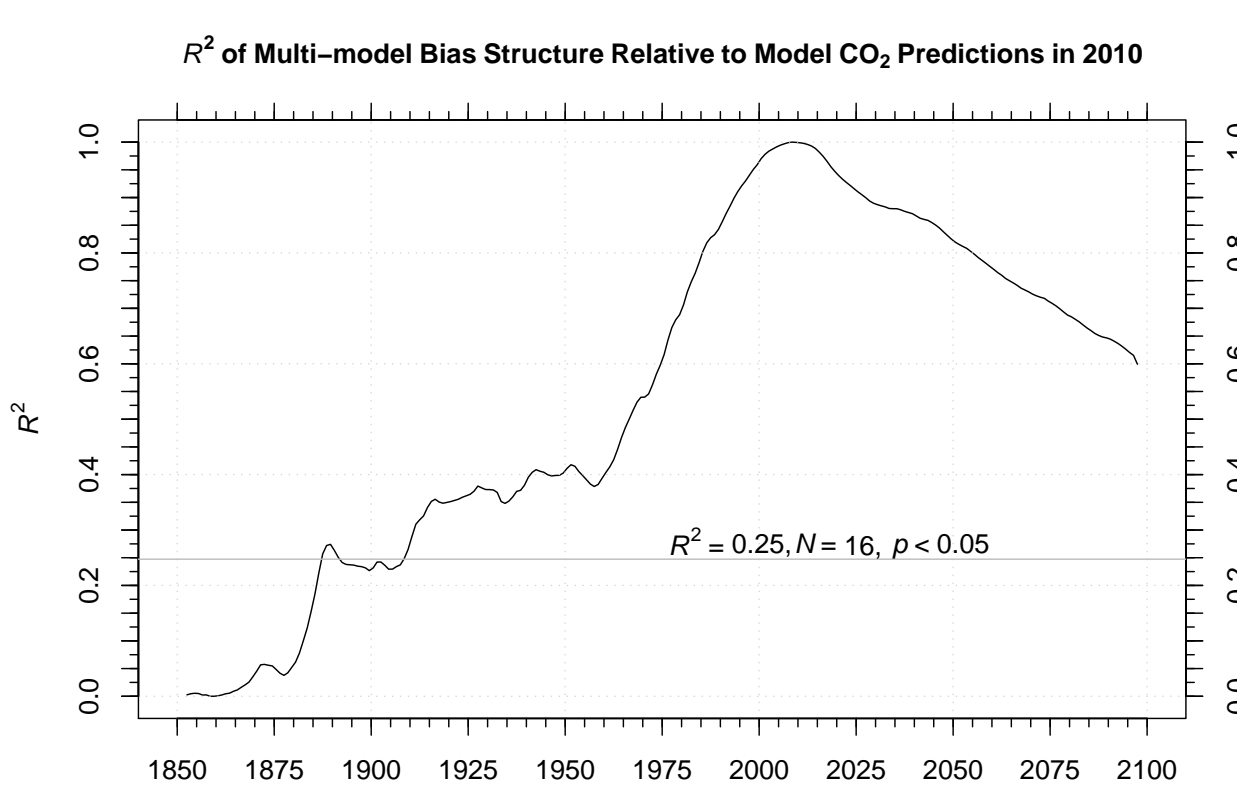


Figure 5: The coefficient of determination ( $R^2$ ) for the multi-model bias structure relative to the set of CMIP5 model atmospheric CO<sub>2</sub> predictions at 2010.

## Implications of a Persistent CO<sub>2</sub> Bias

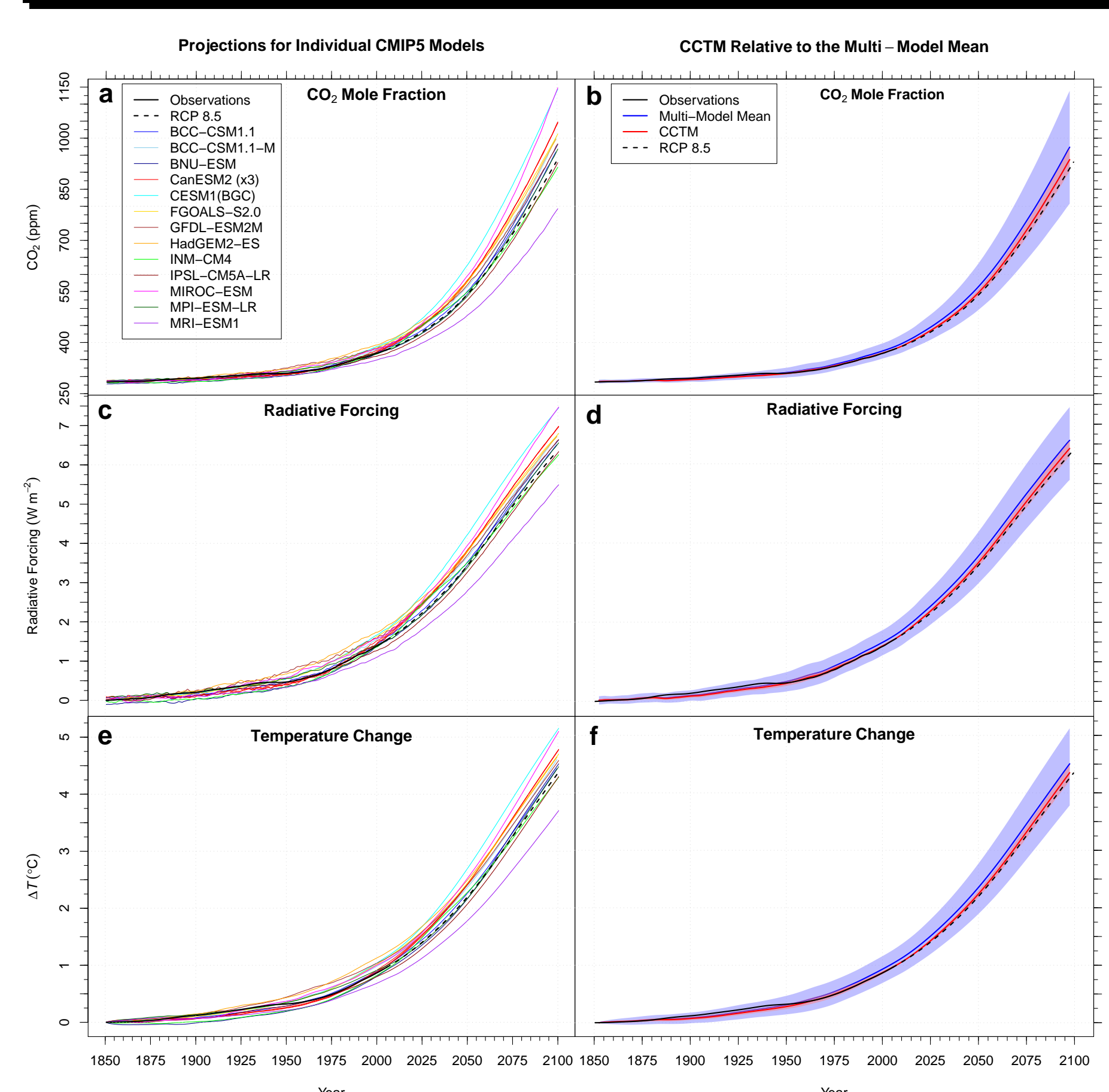


Figure 6: (a) CO<sub>2</sub> predictions for all CMIP5 models. (b) The contemporary CO<sub>2</sub> tuned model (CCTM) atmospheric CO<sub>2</sub> estimate compared to the CMIP5 multi-model mean trajectory. (c and d) Radiative forcing for all CMIP5 models and the CCTM. (e and f) Temperature changes for all CMIP5 models and the CCTM.

Table 2: Atmospheric CO<sub>2</sub> mole fraction, radiative forcing, and resulting temperature changes for each of the CMIP5 ESMs for the years 2010, 2060, and 2100. Values are 5- $y$  means for the time periods 2006–2010, 2056–2060, and 2096–2100.

Model	CO <sub>2</sub> Mole Fraction (ppm)			Radiative Forcing (W m <sup>-2</sup> )			Cumulative ΔT (°C)			ΔT Bias (°C)		
	2010	2060	2100	2010	2060	2100	2010	2060	2100	2010	2060	2100
BCC-CSM1.1	390	603	945	1.70	4.03	6.43	1.06	2.60	4.38	0.03	0.02	0.06
BCC-CSM1.1-M	396	619	985	1.78	4.16	6.65	1.14	2.71	4.54	0.11	0.13	0.22
BNU-ESM	382	602	963	1.59	4.02	6.53	0.98	2.54	4.44	-0.05	-0.04	0.12
CanESM2 r1	394	641	1024	1.75	4.36	6.86	1.07	2.80	4.69	0.04	0.22	0.37
CanESM2 r2	392	641	1023	1.72	4.35	6.85	1.06	2.79	4.69	0.03	0.21	0.37
CanESM2 r3	396	641	1025	1.78	4.35	6.87	1.10	2.80	4.69	0.07	0.22	0.37
CESM1-BGC	407	697	1121	1.92	4.80	7.34	1.21	3.10	5.06	0.18	0.52	0.74
FGOALS-S2.0	404	636	993	1.89	4.31	6.70	1.19	2.75	4.62	0.16	0.21	0.30
GFDL-ESM2G	395	616	967	1.77	4.14	6.56	1.14	2.70	4.50	0.11	0.12	0.18
GFDL-ESM2M	400	621	964	1.83	4.18	6.54	1.18	2.74	4.50	0.15	0.16	0.18
HadGEM2-ES	411	636	983	1.98	4.31	6.64	1.28	2.83	4.58	0.25	0.25	0.26
INM-CM4	386	591	897	1.64	3.92	6.15	1.00	2.57	4.21	-0.03	-0.01	-0.11
IPSL-CM5A-LR	375	573	908	1.48	3.75	6.22	0.93	2.40	4.22	-0.10	-0.18	-0.10
MIROC-ESM	395	658	1121	1.81	4.50	7.35	1.15	2.91	5.00	0.12	0.32	0.68
MIPI-ESM-LR	383	590	948	1.60	3.91	6.45	1.04	2.51	4.39	0.01	-0.07	0.07
MRI-ESM1	361	516	778	1.28	3.20	5.39	0.81	2.05	3.63	-0.22	-0.53	-0.69
Multi-model Mean	393	621	968	1.74	4.19	6.56						